Supporting Information

Facile Preparation of 3D MoS_2/$MoSe_2$ Nanosheets-Graphene Networks as Efficient Electrocatalysts for Hydrogen Evolution Reaction

Shengjie Xu‡, Zhouyue Lei‡ and Peiyi Wu*

State Key Laboratory of Molecular Engineering of Polymers, Collaborative Innovation Center of Polymers and Polymer Composite Materials, Department of Macromolecular Science and Laboratory for Advanced Materials, Fudan University, Shanghai 200433, China.

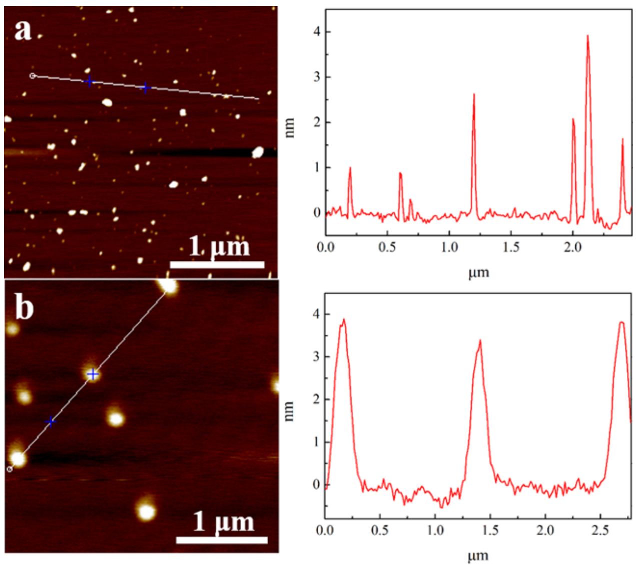

Fig. S1 AFM images of (a) MoS_2 and (b) $MoSe_2$ nanosheets prepared by sonication in NMP. The image (a) is referenced our previous work.[1]

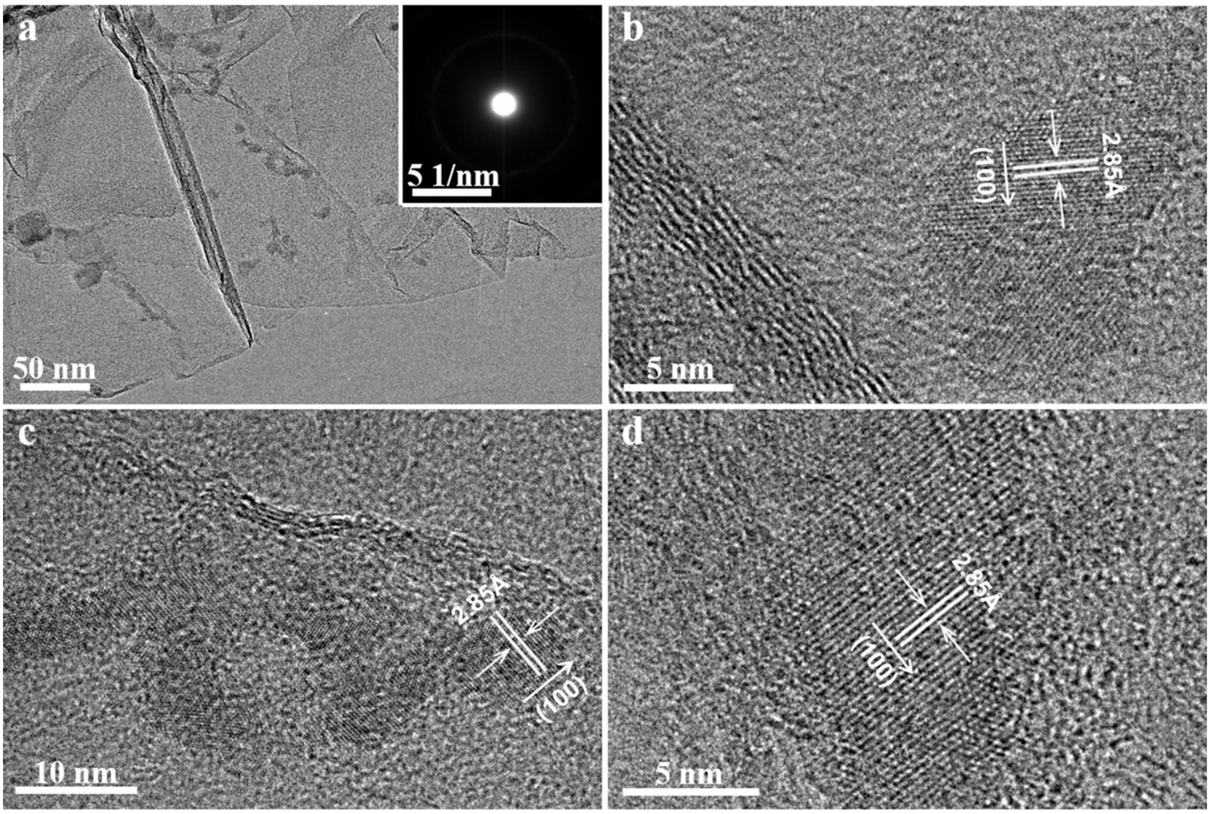

Fig. S2 TEM images of $MoSe_2$-graphene hybrid aerogel ($MoSe_2$-20). (a) smaller size of $MoSe_2$ nanosheets or $MoSe_2$ quantum dots load on RGO sheets; (b), (c), (d) HRTEM images of different area of (a). The inset of (a) is the corresponding SAED pattern.

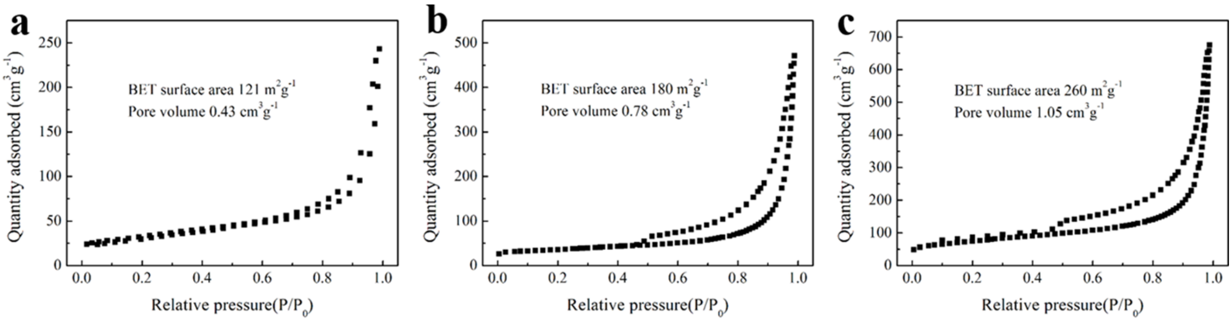

Fig. S3 Nitrogen adsorption-desorption isotherms of pure GA, MoS_2-20, and $MoSe_2$-20.

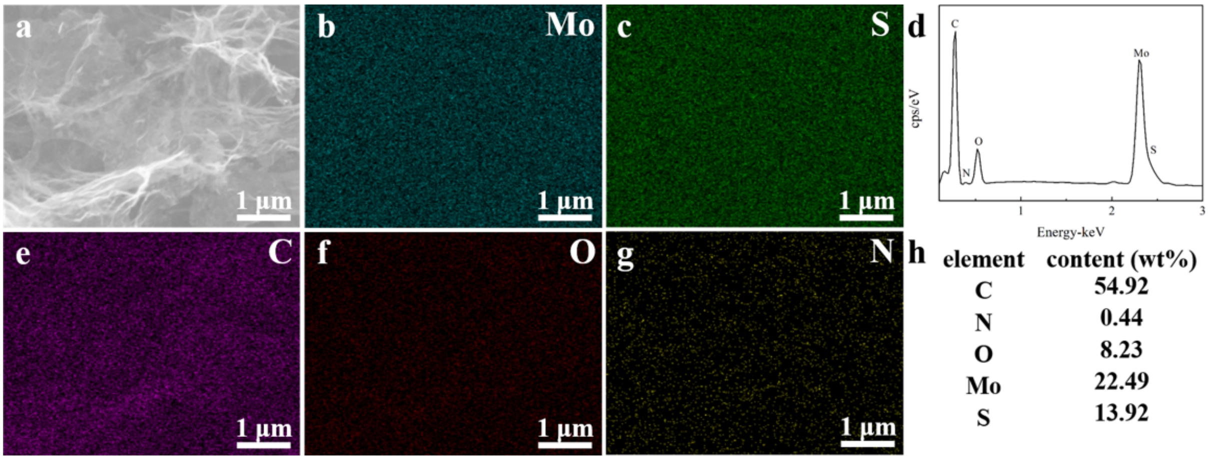

Fig. S4 SEM image, elements mapping images, EDX pattern and the element weight contents of MoS_2-graphene hybrid aerogel (MoS_2-20).

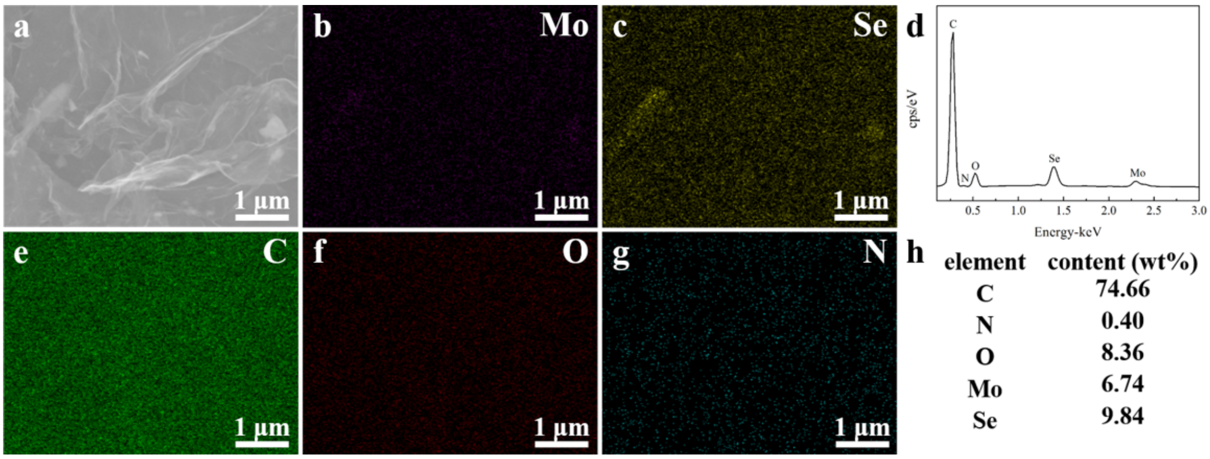

Fig. S5 SEM image, elements mapping images, EDX pattern and the element weight contents of $MoSe_2$-graphene hybrid aerogel ($MoSe_2$-20).

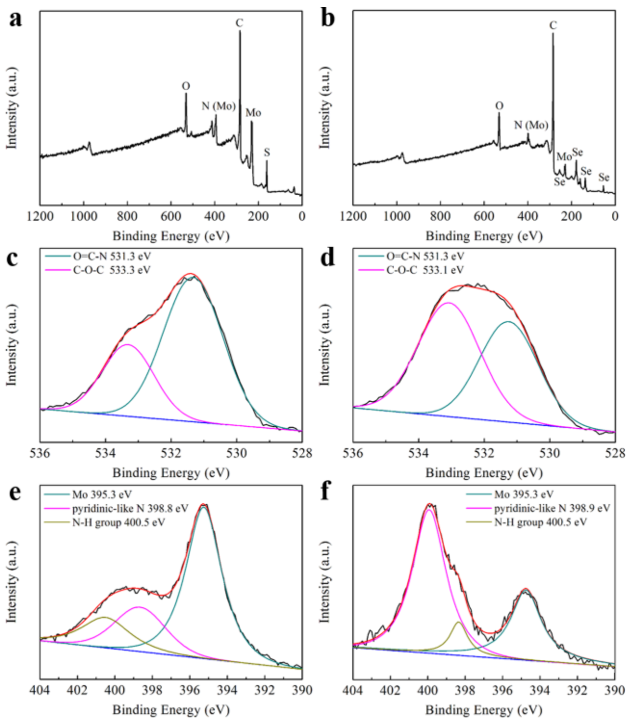

Fig. S6 XPS spectra of MoS_2-20 (left column) and $MoSe_2$-20 (right column) composites. (a) and (b) are XPS spectra; (c) and (d) are the high resolution O_{1s} XPS spectra; (e) and (f) are the high resolution N_{1s} XPS spectra.

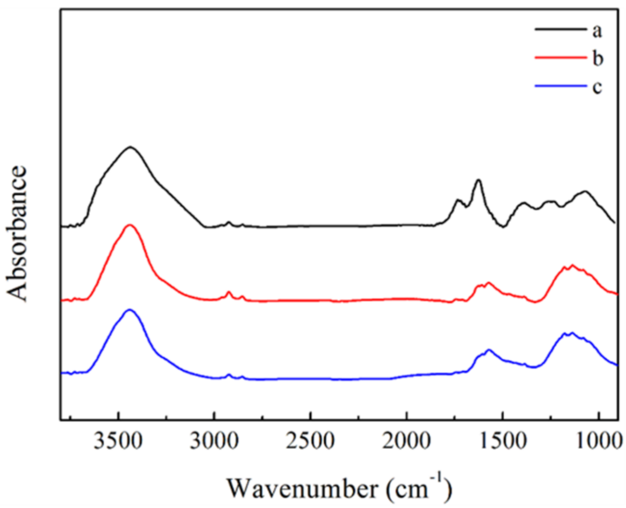

Fig. S7 FTIR spectra of (a) GO, (b) MoS_2-20 and (c) $MoSe_2$-20 composites.

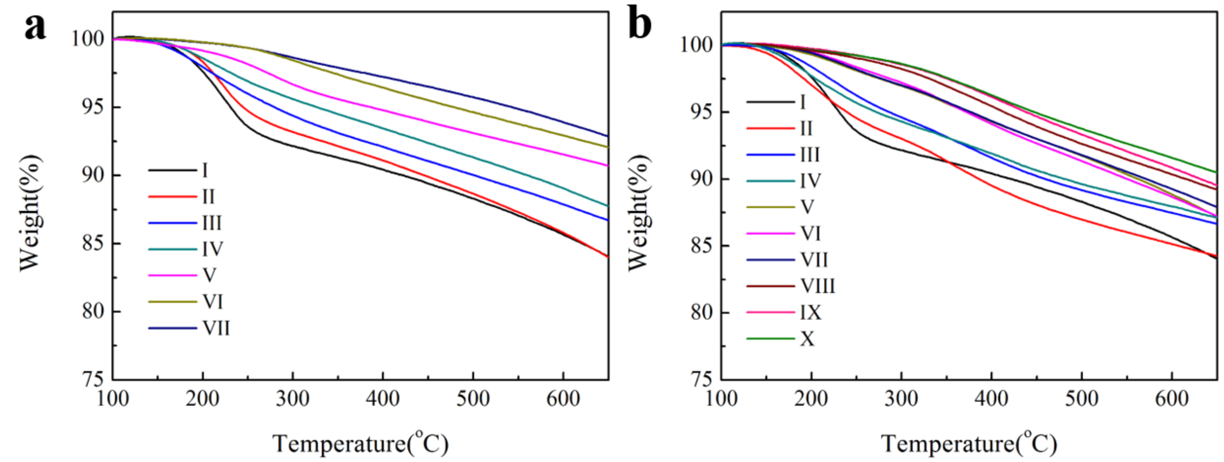

Fig. S8 TGA curves of MoS_2-graphene hybrid aerogels (a) and $MoSe_2$-graphene hybrid aerogels (b) prepared with different dosage of MoS_2 and $MoSe_2$. (I) 0 mL; (II) 1 mL; (III) 3 mL; (IV) 6 mL; (V) 10 mL; (VI) 15 mL; (VII) 20 mL; (VIII) 25 mL; (IX) 30 mL; 40 mL.

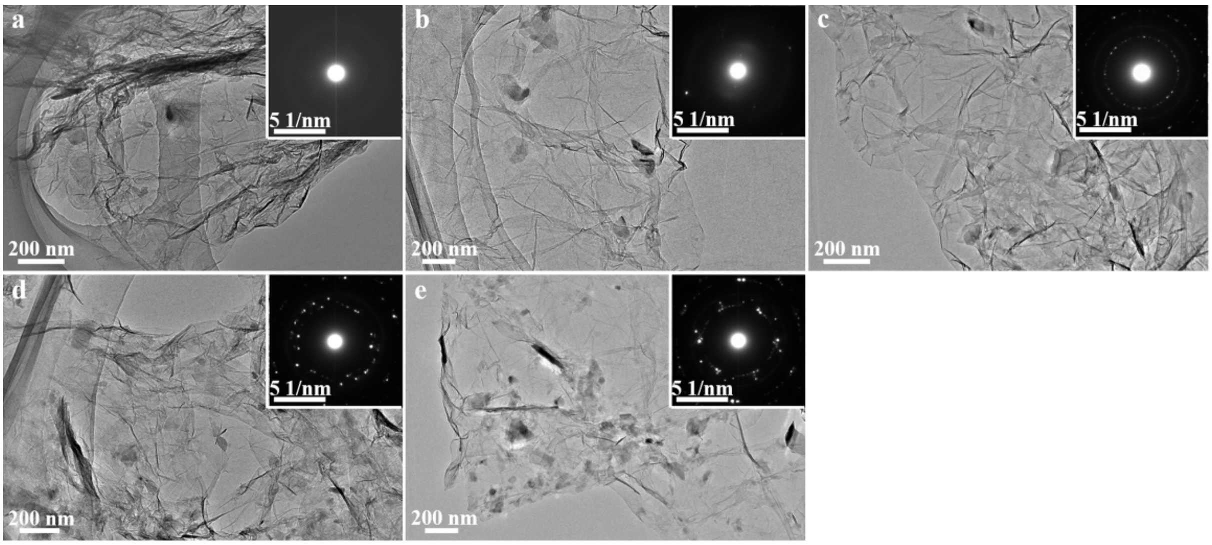

Fig. S9 TEM images of MoS_2-graphene hybrid aerogels prepared with different dosage of MoS_2. (a) 1 mL; (b) 3 mL; (c) 6 mL; (d) 10 mL; (e) 15 mL. The inset is the corresponding SAED pattern of each sample.

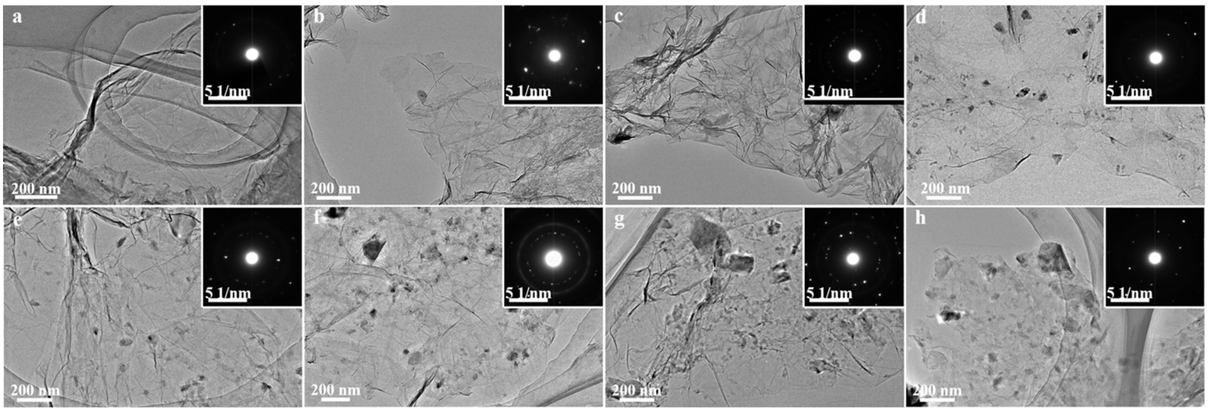

Fig. S10 TEM images of $MoSe_2$-graphene hybrid aerogels prepared with different dosage of $MoSe_2$. (a) 1 mL; (b) 3 mL; (c) 6 mL; (d) 10 mL; (e) 15 mL; (f) 25 mL; (g) 30 mL; (h) 40 mL. The inset is the corresponding SAED pattern of each sample.

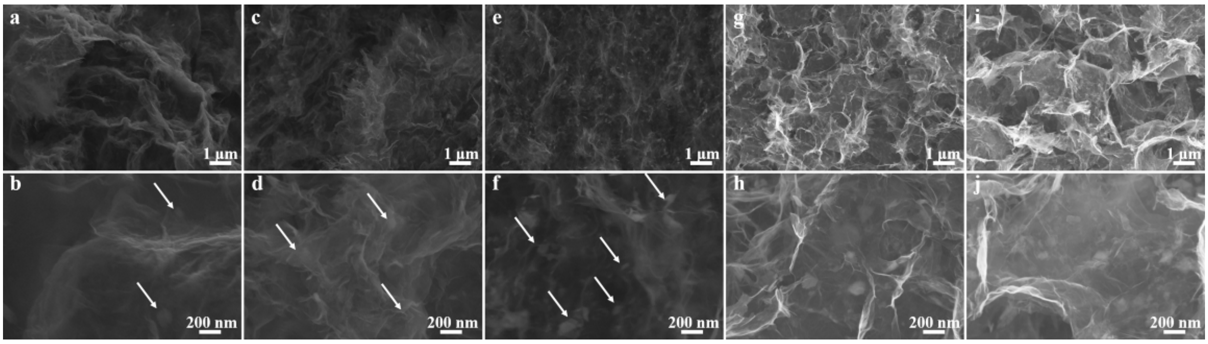

Fig. S11 FESEM images of MoS_2-graphene hybrid aerogels prepared with different dosage of MoS_2. (a) 1 mL; (b) 3 mL; (c) 6 mL; (d) 10 mL; (e) 15 mL. The bottom row are the magnified FESEM of top row.

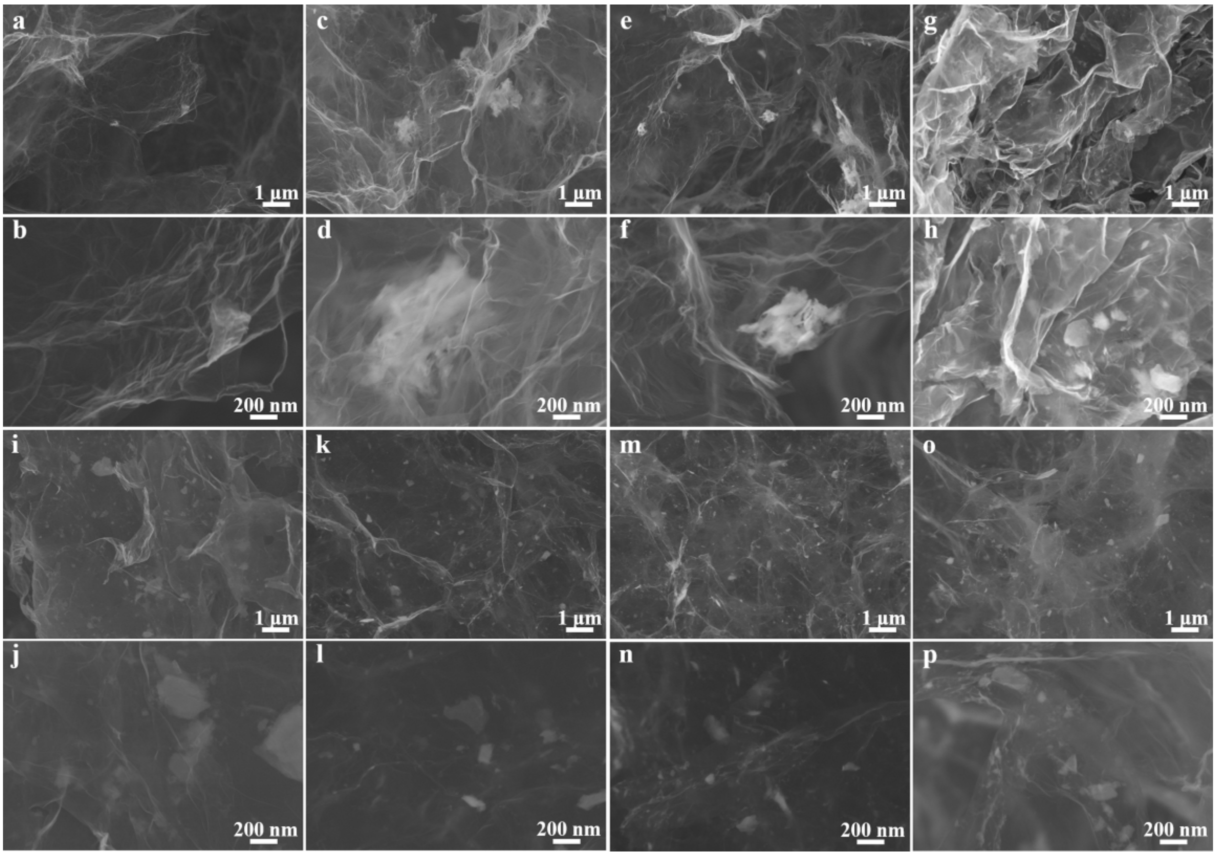

Fig. S12 FESEM images of $MoSe_2$-graphene hybrid aerogels prepared with different dosage of $MoSe_2$. (a) 1 mL; (b) 3 mL; (c) 6 mL; (d) 10 mL; (e) 15 mL; (f) 25 mL; (g) 30 mL; (h) 40 mL.

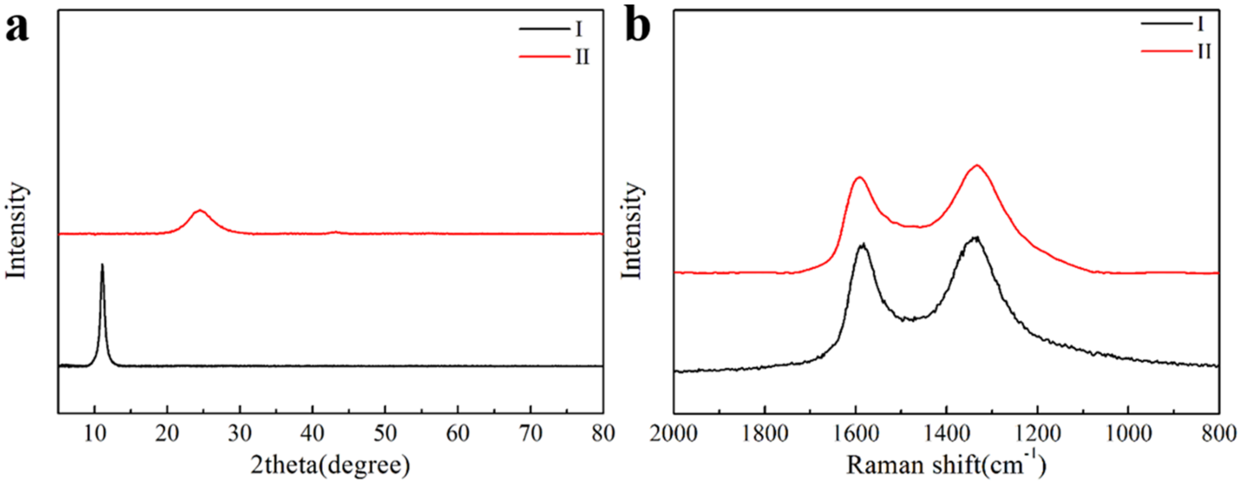

Fig. S13 XRD patterns (a) and Raman spectra (b) of GO (I) and graphene aerogel (II).

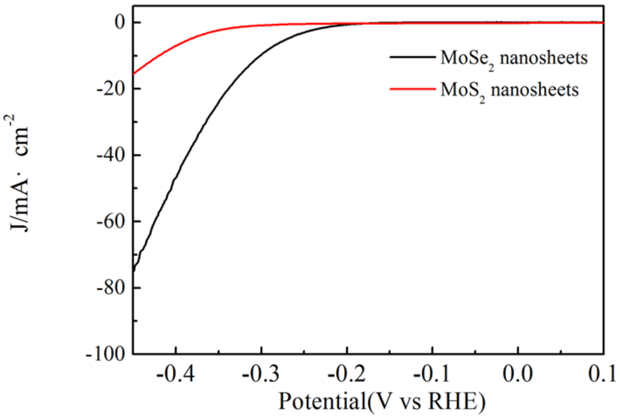

Fig. S14 Polarization curves of MoS_2 and $MoSe_2$ nanosheets.

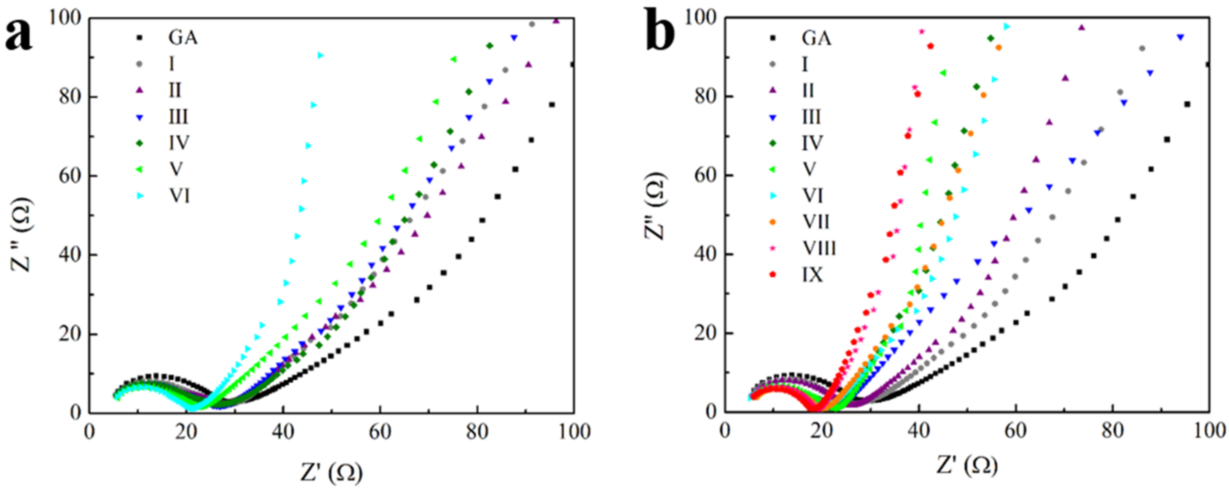

Fig. S15 Nyquist plots of MoS_2-graphene hybrid aerogels (a) and $MoSe_2$-graphene hybrid aerogels (b) prepared with different dosage of MoS_2 and $MoSe_2$. (I) 1 mL; (II) 3 mL; (III) 6 mL; (IV) 10 mL; (V) 15 mL; (VI) 20 mL; (VII) 25 mL; (VIII) 30 mL; (IX) 40 mL.

The charge-transfer resistances (R_{ct}) were determined by fitting the impedance spectra using the Z-view software, and in all cases it achieved good agreement between the measured and the fitted data. The charge-transfer resistances were summarized in Table. S1 (MoS_2-graphene hybrid aerogels) and Table. S2 ($MoSe_2$-graphene hybrid aerogels).

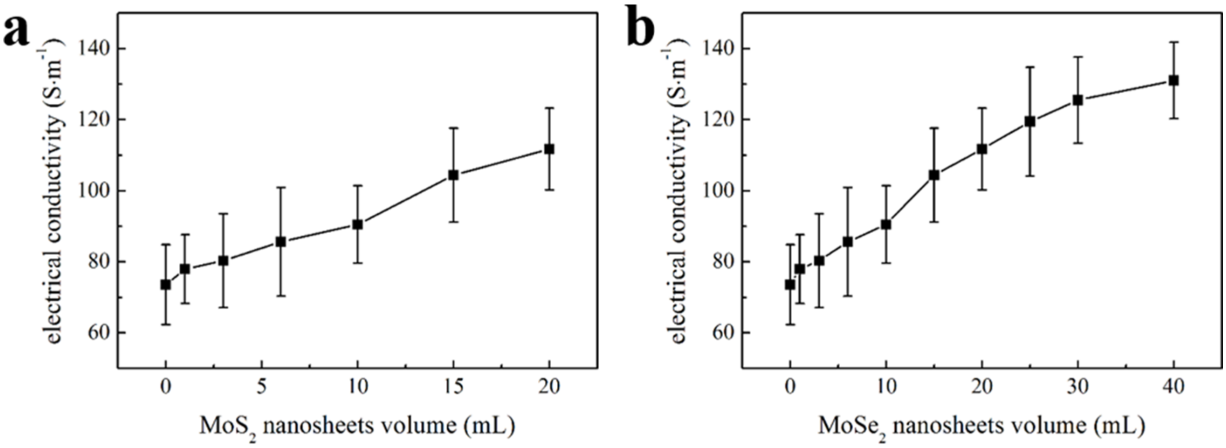

Fig. S16 Electrical conductivity of MoS_2-graphene hybrid aerogels (a) and $MoSe_2$-graphene hybrid aerogels (b) prepared with different dosage of MoS_2 and $MoSe_2$.

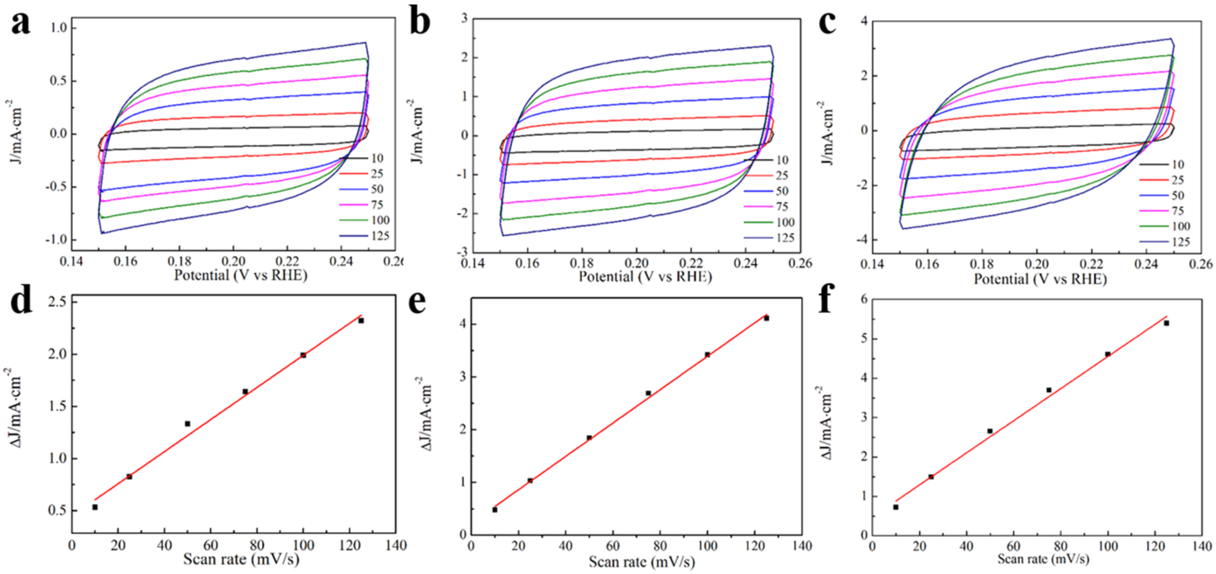

Fig. S17 Typical CV curves (top row) and corresponding differences in the current density at 0.2 V plotted against scan rate (bottom row). (a) and (d) are corresponding to the graphene aerogel, (b) and (e) are corresponding to MoS_2-20, (c) and (f) are corresponding to $MoSe_2$-20.

We calculated the electrochemical active surface areas of the as-prepared catalysts by measuring their electrochemical double layer capacitances (C_{dl}) using a simple CV method according to previous reports.[2, 3] In brief, capacitance measurements were performed in a potential range of 0.15-0.25 V vs RHE since there was no obvious electrochemical feature corresponding to Faradic current observed in this region for each catalyst. And the capacitive currents, i.e. ΔJ@0.2 V, were then plotted as a function of CV scan rate. It was observed a linear relationship in which the slope twice larger than the C_{dl} Value. And C_{dl} and electrochemical active surface area values were summarized in Table. S1 (MoS_2-graphene hybrid aerogels) and Table. S2 ($MoSe_2$-graphene hybrid aerogels).

Table. S1 Summary of the charge-transfer resistance, C_{dl} and electrochemical active surface area values of graphene aerogel and MoS_2-graphene hybrid aerogels.

Samples	Charge-transfer resistance (Ω)	C_{dl} (mF cm^{-2})	Electrochemical active surface area (cm^2)
Graphene aerogel	25	5.4	19
MoS_2-1	23	6.3	22
MoS_2-3	20	8.9	31
MoS_2-6	20	9.6	34
MoS_2-10	19	11.1	39
MoS_2-15	18	12.5	44
MoS_2-20	17	15.8	56

Table. S2 Summary of the charge-transfer resistance, C_{dl} and electrochemical active surface area values of $MoSe_2$-graphene hybrid aerogels.

Samples	Charge-transfer resistance (Ω)	C_{dl} ($mF\ cm^{-2}$)	Electrochemical active surface area (cm^2)
$MoSe_2$-1	22	6.9	24
$MoSe_2$-3	21	8.6	30
$MoSe_2$-6	19	10.8	38
$MoSe_2$-10	19	14.3	50
$MoSe_2$-15	18	19.1	67
$MoSe_2$-20	16	20.4	72
$MoSe_2$-25	16	24.5	86
MoS_2-30	15	28.4	100
$MoSe_2$-40	14	31.5	111

References

1. S. Xu, D. Li and P. Wu, *Adv. Funct. Mater.*, 2015, **25**, 1127-1136.
2. Y. Zheng, Y. Jiao, L. H. Li, T. Xing, Y. Chen, M. Jaroniec and S. Z. Qiao, *ACS Nano*, 2014, **8**, 5290-5296.
3. E. Navarro-Flores, Z. Chong and S. Omanovic, *J. Mol. Catal. A-Chem.*, 2005, **226**, 179-197.